Polymer 51 (2010) 1703–1708

Contents lists available at ScienceDirect

Polymer

journal homepage: www.elsevier.com/locate/polymer

Preparation of macroporous monolith with three dimensional bicontinuous skeleton structure by atom transfer radical polymerization for HPLC

Rongyue Zhang [a,b], Li Qi [a,*], Peiyong Xin [a,b], Gengliang Yang [c], Yi Chen [a]

[a] Beijing National Laboratory for Molecular Sciences, Key Laboratory of Analytical Chemistry for Living Biosystems, Institute of Chemistry, Chinese Academy of Sciences, Beijing 100190, China
[b] Graduate School, Chinese Academy of Sciences, Beijing 100049, China
[c] College of Pharmacy, Hebei University, Baoding 071002, China

ARTICLE INFO

Article history:
Received 4 November 2009
Received in revised form
21 January 2010
Accepted 1 February 2010
Available online 16 February 2010

Keywords:
Three dimensional bicontinuous skeleton
Monolith
ATRP

ABSTRACT

A three diamensional (3D) bicontinuous skeleton macroporous monolith was firstly prepared by *in situ* atom transfer radical polymerization (ATRP) of ethylene glycol dimethacrylate (EDMA) at the room temperature. The structure of the monolith could be mediated by the different ratio of EDMA to initiator and the 3D bicontinuous skeleton structure was obtained at the ratio of 70:1. Compared with the traditional monoliths prepared by conventional free radical polymerization, the monolith made of ATRP could be trended to form the 3D bicontinuous skeleton macroporous structure, due to low concentration of free radical and the step-wise growth of polymer chains in ATRP. The diameter of the monolith could be enlarged to 50 mm without obvious volume shrink and cracks in the body. The morphology and pore distribution of the monolith were characterized by SEM and mercury intrusion porosimetry. The monolith was modified by grafting polymerization of n-butyl methacrylate, and then the grafted monolith was used to separate some steroids and proteins by reversed-phase liquid chromatography.

1. Introduction

Over the past two decades, there has been significant interested in development of preparation of rigid porous polymer monoliths by *in situ* method [1,2]. This method is a simple molding process carried out within the confines of a closed mold, in which polymerization of a mixture comprising monomers, initiator, and porogenic solvent affords macroporous materials with large through-pores that enable applications in a rapid flow-through mode. The pores in the monoliths are fabricated by phase separation between polymers and porogenic solvent induced by polymerization without any stir. Generally, the vinyl monomers and cross-linkers of conventional free radical polymerization (CFRP) are used to prepare the rigid porous monolith. In this method, the growing polymer chains tend to aggregate each other because van der Waals attraction surmounts the steric hindrance mutually expelling the polymer chains [3], and the segregated polymer chains soon form tiny particles, then those particles aggregate to the typical heterogeneous macroporous structures composed of micron size global particles [4,5]. The inherent disadvantages of these heterogeneous macroporous monoliths are cited by the adverse effects such as larger eddy diffusion resulted from irregular interstitial channels, lower permeability, compressibility at high-pressure drops [6].

In order to change the heterogeneous structures of polymer monoliths, some researchers have made efforts to develop special studies on other typical preparation methods for preparation of three dimension (3D) bicontinuous skeleton macroporous monoliths. Hosoya and colleagues prepared the epoxy-based monoliths with 3D bicontinuous structure through a polycondensation reaction with an epoxy compound and an amino compound [7–9]. Kanamori and co-workers reported that the 2,2,6,6-tetramethylpiperidin-1-yl oxide (TEMPO)-mediated living radical polymerization was used to afford 3D bicontinuous structure monoliths [10]. Additionally, Aoki and colleagues presented that ultra high molecular weight poly(styrene) as porogen was used to induce viscoelastic phase separation, which afforded monoliths with unusual pores [11]. In our previous work, a high internal phase emulsion (HIPE) polymerization was used to prepare the monolith with sub-micron skeletons and well-defined macropores [12]. Although the above methods could afford 3D bicontinuous structure monoliths, there were still some limitations, such as few

* Corresponding author. Institute of Chemistry, Chinese Academy of Sciences, Zhongguancun North First Street 2#, Beijing 100190, China. Tel.: +86 10 82627290; fax: +86 10 62559373.
E-mail address: qili@iccas.ac.cn (L. Qi).

0032-3861/$ – see front matter © 2010 Elsevier Ltd. All rights reserved.
doi:10.1016/j.polymer.2010.02.002

monomers chosen for *in situ* polycondensation reaction, the high temperature (130 °C) needed by TEMPO-mediated living radical polymerization and a lot of experimental operations for HIPE. Therefore, research on a simple and mild method for preparation 3D bicontinuous structure monolith has been concerned in recent years.

Atom transfer radical polymerization (ATRP) has been extensively applied to synthesizing or modifying materials [13–17]. Some studies indicate that polymer gels prepared by ATRP are homogeneous in comparison with CFRP [18]. In ATRP, the concentration of propagating radical is low during polymerization, and thus, it often takes hours for an individual chain to propagate hundreds of monomer units and chains growth through propagation is slowed down. However, only seconds for the same number of monomer units are needed to be added to the polymer chain in CFRP while the process of chain relaxation would need minutes or hours. This mismatch in rates results in the formation of highly cross-linked microdomains distributed across the whole network. Therefore, these high local concentration fluctuations in microcosmic size tend to form the particle-aggregation structure of monolith by CFRP. In the contrary, the slow chain growth and negligible chain transfer in ATRP are expected to form the homogeneous structure of monolith. It has been reported that ATRP of 1,3-glycerol dimethacrylate afford a monolith with well-defined bicontinuous structure at 70 °C [19].

In this study, we make an attempt to prepare monolith with 3D homogenous structure by ATRP of ethylene glycol dimethacrylate at the room temperature and apply it to use as a stationary phase of HPLC for separation of steroids and proteins.

2. Experimental section

2.1. Chemicals

Ethylene glycol dimethacrylate (EDMA) and n-butyl methacrylate (BMA) were purchased from Acros company (New Jersey, USA) and purified before use. Azobisisobutyronitrile(AIBN) was produced by Shanghai Chemical Plant (Shanghai, China) and refined by recrystallization from the methanol before use. CuBr (Beijing Chemical Plant, Beijing, China) was firstly washed by acetic acid for 24 h and subsequently washed by methanol before use. *N*,*N*,*N*′,*N*″,*N*‴-pentamethyldiethylenetriamine (PMDETA) was purchased from JK Chemical Ltd (Tokyo, Japan). Ethyl-2-bromopropionate (EBP) and ascorbic acid were obtained from Alfa Aesar (Lancs, England). Methanol, hexane, tetrahydrofuran (THF) and $CuBr_2$ were purchased from Beijing Chemical Plant (Beijing, China). All the above chemicals were received. The steroids were purchased from Wuhan Jiuan Pharmaceutical Ltd (Hubei, China). The four test proteins, cytochrome *c*, myoglobin, ribonuclease A and ovalbumin were obtained from Sigma–Aldrich company (Louis, USA).

2.2. Preparation of the monolith

In a typical polymerization, EDMA (5.0 mL, 2.6 mmol), EBP (4.7 μL, 0.037 mmol), CuBr (5.3 mg, 0.037 mmol), methanol (5.0 mL) and hexane (5 mL) were added to a dry ampule. The ampule was then sealed with a rubber septum and degassed with ultrahigh-purity nitrogen for 20 min. Deoxidized PMDETA (7.7 μL, 0.037 mmol) was quickly added to the ampule by a degassed syringe. The ampule was shaken for 30 s; then the reaction mixture was injected into the stainless steel chromatographic columns. The columns filled with reaction mixture were quickly sealed with rubber septa covered with pieces of polyethylene film. The polymerization was allowed to proceed at the room temperature of 20 °C for 24 h, the seals were removed, and the column was provided with fittings and attached to the HPLC system. 100 mL THF was pumped through the monolith at a flow rate of 0.20 mL/min to remove the porogenic solvents and other soluble compounds that remained in the polymer rod after the polymerization was completed. Then a 50 mL water was pumped through the monolith at a flow rate of 0.50 mL/min in order to remove copper ion remaining in the monolith. At last, 50 mL mixture of methanol and hexane (1/1, v/v) was pumped through the monolith at a flow rate of 0.50 mL/min for the following modification of the monolith.

2.3. Modification of the monolith

A typical graft copolymerization was implemented using surface-initiated activators generated by electron transfer atom transfer radical polymerization (AGET ATRP) [20] and the polymerization procedure was similar with the previous report [21]. The detailed process was described as follows: $CuBr_2$ (8.26 mg, 0.037 mmol), PMDETA (7.7 μL, 0.037 mmol) and BMA (5 mL, 31 mmol) in the combined solvent of methanol and hexane (50 mL, 1:1, v/v) were added into a flask followed by well mixing under ultrasound. Subsequently, the ascorbic acid aqueous solution (1.0 mL, 0.16 mol/L) was injected into the flask with a syringe. The resulting mixture was pumped through the prepared monolith by syringe pump at a flow rate of 0.10 mL/min and reacted for 10 h at 20 °C. After the grafting copolymerization was completed, 100 mL THF was used to wash the monolith for removing all soluble compositions that were present in the monolith. Then 50 mL water was pumped through the grafted monolith for removing copper ion remaining in the column. The above process was repeated at different reaction time.

2.4. Characterization of the monolith

The monoliths in the columns were pumped out and cut into small pieces followed by drying under vacuum at 20 °C for 48 h. Microstructures of the dried monolith samples were observed by scanning electron microscopy (SEM, Hitachi S-4300 and S-4800, Japan, operated at 10 kV). The pore size distribution was determined by mercury intrusion porosimetry on a PoreMasterGT and by nitrogen adsorption porosimetry. Transmission infrared spectrum were obtained from RFS100/S (Bruker, Germany). Chromatographic experiments were carried out with a Shimadzu LC-20A HPLC system (Shimadzu, Japan) consisting of a binary LC-20AT HPLC pump and an SPD-20A UV–Vis detector. Data processing was performed with an HW-2000 chromatography workstation (Nanjing Qianpu Software, China).

Table 1
Preparation conditions of the monoliths.

Monolith	EDMA (mmol)	EPB (mmol)	CuBr/PDMETA (mmol/mmol)	AIBN (mmol)	Temperature (°C)	Time (h)	Tatal pore area (m^2/g)	Total pore volume(mL/g)
M(a)	2.6	2.6	2.6/2.6	0	20	24	29	1.2
M(b)	2.6	0.13	0.13/0.13	0	20	24	19	1.3
M(c)	2.6	0.037	0.037/0.037	0	20	24	28	1.4
M(d)	2.6	0.037	0/0.037	0.037	60	24	20	1.3
M(e)	2.6	0.037	0.037/0.037	0	60	24	32	1.5

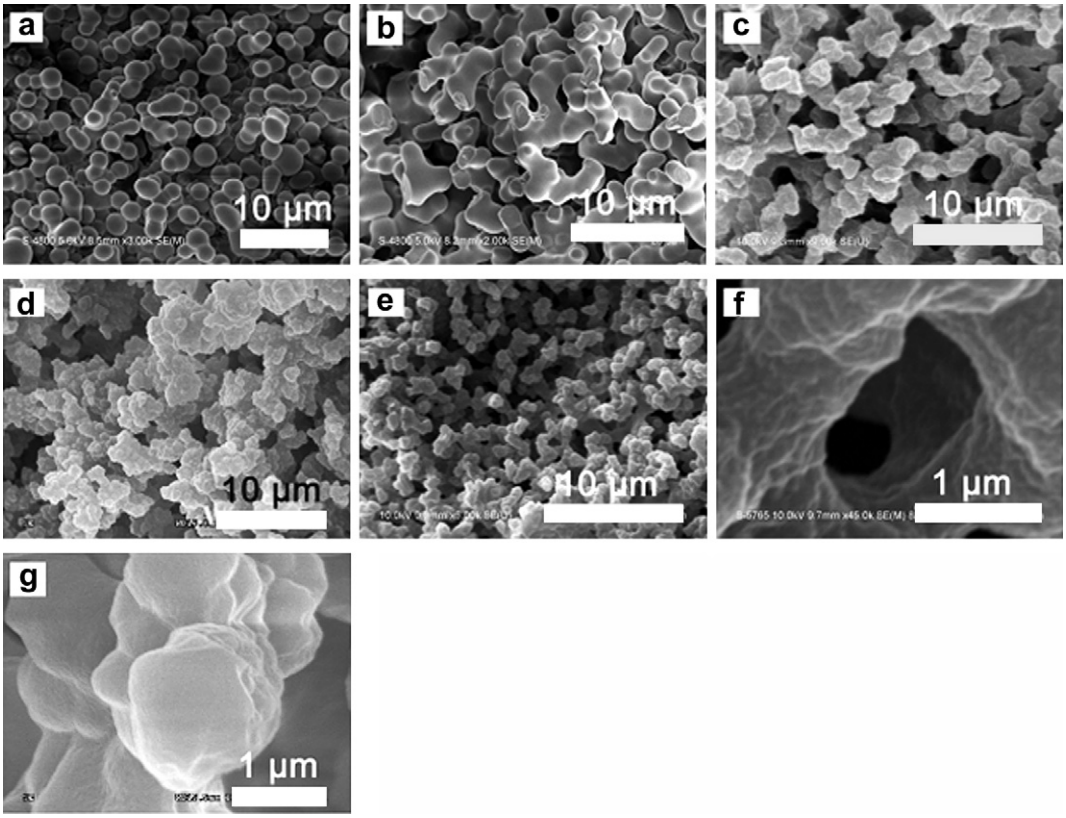

Fig. 1. SEM images of the monoliths (a, b, c, d and e are M(a), M(b), M(c), M(d) and M(e) in Table 1, f and g are the magnified local of the c and d, respectively).

3. Results and discussion

3.1. Preparation of 3D monoliths

There are many factors that have influenced on morphology of monoliths, which include functional monomers and cross-linkers [22], types of porogen [23] and polymerization temperature [24,25]. Those factors mentioned above have been studied in preparation of monoliths by CFRP in literatures. However, an important factor that affects gel point in preparation of gelation by living polymerization is rarely studied in preparation of monoliths, which is the ratio of cross-linker to initiator (RCI), a critical role in preparing a 3D monolith [26]. In this study, the polymerization

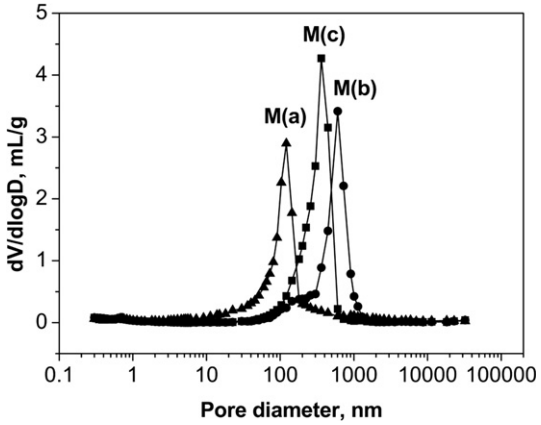

Fig. 2. Pore size distribution profiles for the monolith by mercury intrusion porosimetry. (▲,M(a); ●,M(b); ■,M(c) in Table 1).

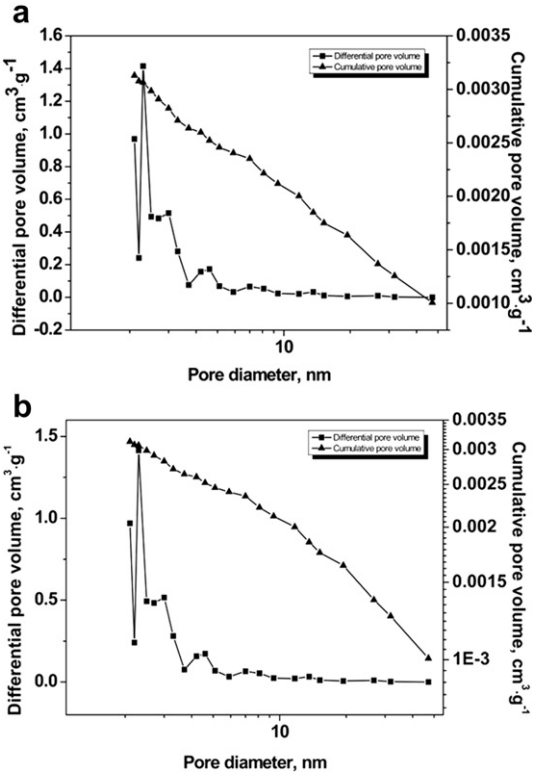

Fig. 3. Pore size distribution profiles for M(a)((a)) and M(c)((b)) by nitrogen adsorption porosimetry. (M(a) and M(c) in Table 1).

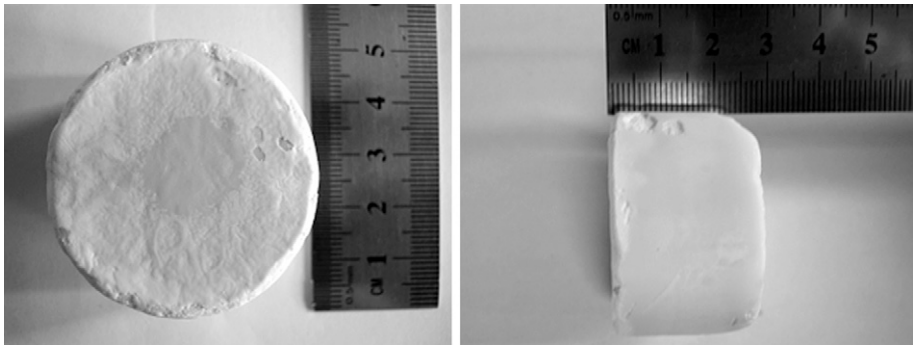

Fig. 4. Photographies of the large size of the monoliths. (CuBr/EPB/PMDETA/EDMA = 0.13/0.13/0.13/8.8 mmol; EDMA/Methanol/Hexane = 17/17/17 mL; 24 h, 20 °C).

system was composed of EDMA that was selected as the sole reactive component, porogen including methanol and hexane, CuBr, EBP and PMDETA (Table 1). The effect of RCI (mol ratio) in the range of 100:1-1:1 on morphology of the monolith was emphatically studied while the other reaction conditions kept constant. The SEM images of different RCI ratios are then investigated in Fig. 1.

Fig. 1a shows that monolith by the RCI of 1:1 affords 2–3 μm dispersive particles. It illustrated that low RCI led to high rate of crosslink polymerization which caused earlier microgels, and these microgels adsorbed monomer to increase their sizes, and subsequently, the bigger particles aggregated to form the aggregated particles structure. When the RCI increased to 20:1, the 2–3 μm dispersive particles began to aggregate to form a sole skeleton (Fig. 1b). It can be inferred that decrease of concentration of initiator reduce the rate of crosslinking polymerization, which delayed the formation of microgels in the polymerization system. However, when the value of RCI reached 70:1, the aggregated particles disappeared and the obvious 3D structure appeared in the monoliths (Fig. 1c).

The pore diameter distributions of M(a), M(b) and M(c) were characterized by mercury intrusion porosimetry (Fig. 2). The results indicated that M(a) had 1.1 μm median pore and the average pore diameter of 159.5 nm which were smaller than 3.4 μm median pore and 193.3 nm average pore diameter of M(c), respectively. M(b) had 6.1 μm median pore and the average pore diameter was 239.5 nm. As a result, the total surface area of M(b) was 19 m^2/g, and the low surface area was turned against the separation. The mesopores and micropores of M(a) and M(c) were determined by nitrogen adsorption porosimetry and the results showed that their micropores distribution centred round 1.8–2.0 nm and mesopores (2–50 nm) had less percent as shown in Fig. 3a and Fig. 3b. Besides, it seemed that different RCI had less effect on formation of micropores and mesopores in monolith. At the same flow rate, the backpressure of M(c) was obvious lower than one of M(a) when the two monoliths were connected to HPLC. Considering the better permeability of M(c), the M(c) was used to complete the following grafting polymerization.

3.2. Mechanism of 3D bicontinuous skeleton structure monoliths

What was the dominating role at forming 3D bicontinuous skeleton structure? To explore this question, the control monolith (M(d) in Table 1) was prepared by CFRP. The polymerization was the same but CuBr was replaced with AIBN and the temperature increased to 60 °C. However, another different structure is investigated (Fig. 1d). It displayed that the skeletons were composed of the aggregated particles and the pores were formed by the voids between the aggregated particles. As M(d) was prepared at 60 °C, a compared experiment was thus designed at the same temperature (M(e) in Table 1). Fig. 1e exhibits that M(e) still keeps the 3D structure except that the size of skeleton of M(e) changes slightly smaller than the one of M(c). This phenomenon is the same as described in reference [26]. In order to better observe the difference between the 3D bicontinuous skeleton of the M(e) and the aggregated particles structure of M(d), the local pore and skeleton of the M(e) and M(d) are magnified by SEM and shown in Fig. 1f and g, respectively. Fig. 1f demonstrates that the local skeleton and pores of M(e) is a kind of 3D network skeleton structure, in the contrary, Fig. 1g shows that the skeletons of M(d) are formed by the connected global particles and the pores are formed by the void among the connected global particles.

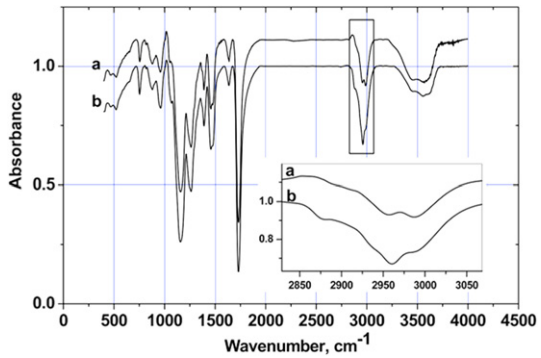

Fig. 5. FT-IR spectrums of the ungrafted (a) and the grafted monolith (b).

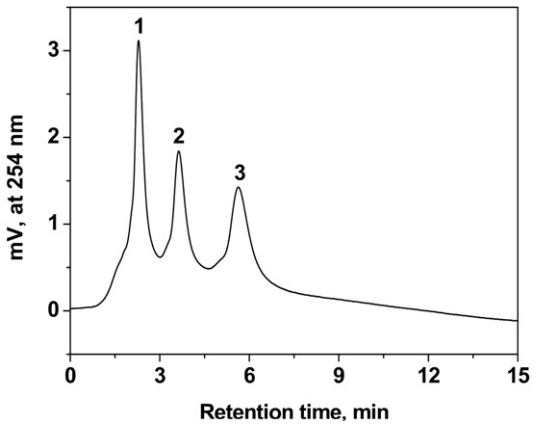

Fig. 6. Chromatograms of separation of three steroids on the grafted monolith. 1, hydrocortisone; 2, testosterone; 3, progesterone. Conditions: grafted monolithic column, 50 × 4.6 mm i.d.; mobile phase, 30% methanol in water; flow rate, 1 mL/min; detection, UV at 254 nm.

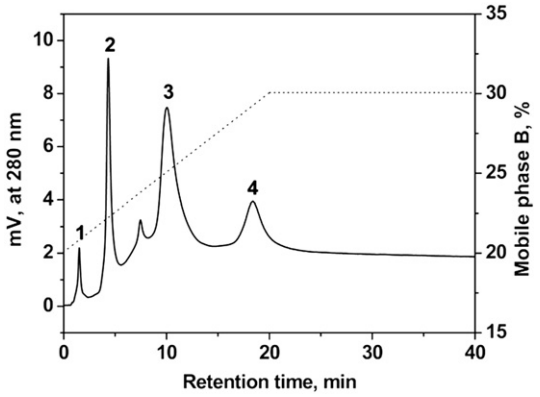

Fig. 7. Chromatograms of a four-protein mixture on the grafted monolith. Conditions: grafted monolithic column, 50 × 4.6 mm i.d.; mobile phase A, 0.1% TFA solution; mobile phase B, actronile-water 0.1% TFA solution (30:70, v/v); step gradient, 100% A to 100% B in 20 min; flow rate, 1 mL/min; detection, UV at 280 nm. Peaks: 1, ribonuclease; 2, cytochrome *c*; 3, myoglobin; 4, ovalbumin.

These results suggested that the mechanism of ATRP seemed to play an important role in forming 3D bicontinuous skeleton structure of the monolith.

The possible reasons were as follows:

(1) In CFRP, the reaction more effectively proceeds on the sites of the species that have already started to polymerize while leaving considerable less-reacted and unreacted species. These lead to a high polymer diffusion index (PDI) resulting in a hetergenous networking structure. On the contrary, ATRP allows the homogenous branching resulting from the highly homogeneous reaction ideally without a termination reaction, which affords a lower PDI of the growing species, therefore, it is forward to form homogenous 3D skeleton structure.
(2) In ATRP, the lengths of polymer chains gradually grow in a step-wise manner and the rapid segregation of microgel is effectively suppressed. This is due to driving toward delaying the phase separation in the polymerization.
(3) Additionally, some reports on preparation of the monoliths by living polymerization [7–9] or polycondensation [10] had pointed out that the low polymerization rate and the way of the step-wise growth of the polymer chains tended to form 3D bicontinuous skeleton structure of the monolith.

Therefore, the low concentration of free radical and the step-wise growth of polymer chains in ATRP might make an important effect on preparing the 3D bicontinuous skeleton structure of the monolith, which is different from CFRP. Besides, the inherent phenomena of the free radical polymerization in CFRP, such as higher exothermic reaction at elevated temperatures, strong autoacceleration (gel effect) and the termination reaction affecting functional group reactivity, make the monolith structure more heterogeneous and the monolith volume limited to be a relatively small value. For example, 100 × 4.6 mm i.d. and 50 × 4.6 mm i.d. steel columns or capillary column were used to be mold for preparation of the monolith. To get a bigger-volumed monolithic column, some special operations were needed to help diffuse the reaction thermo [27,28]. In this study, the general process by ATRP was used to prepare the monolith and the volume of the monolith could be enlarged to 50 mL. Fig. 4 illustrates that the diameter and length of the large volume monolith were 50 mm and 28 mm, respectively. Considering the cost of monomers, the further enlarging experiment did not be carried out in this study. This large-volumed monolith could be expected to be used in preparative chromatography.

3.3. Modification of the monolith

It is well known that surface-initiated ATRP is used to modify the surface of materials [29–31]. Furthermore, to get a hydrophobic surface, BMA was grafting polymerized from the surface of internal pores of the monoliths, as the group of bromine in the surface of the monolith could initiate ATRP of vinyl monomer. The process of grafting polymerization was similar with our previous work [22]. In order to guarantee the permeability of the grafted monolith for application in HPLC, the grafting polymerization time was investigated from 5 h to 20 h. The backpressures of the monoliths by different grafting polymerization time were determined by HPLC at different flow rates and showed an increase trend with the increase of the grafting polymerization time. The reason was that the longer polymerization time would lead to the longer length of the grafted polymer chains, which would cause the bigger resistance to flow of the mobile phase through the monolith. Although shorter grafting polymerization time would result in the higher permeability, the shorter length of the grafted PBMA in the surface of the grafted monolith was obtained with lack of enough hydrophobility for separation of analytes. Therefore, the 15 h polymerization time was chosen to be the ideal reaction time. The backpressure of the grafted monolith by 15 h was only 0.9 MPa at the flow rate of 1.0 mL/min when water was used to be a mobile phase. This result indicated that the grafted monolith had good permeability.

Additionally, the grafted monolith was characterized by FT-IR. Fig. 5 displays that $-CH_3$ (2960.91 cm^{-1} and 2875.88 cm^{-1}) in PBMA units in spectrum b (grafted monolith) is strengthened in compared with spectrum a (ungrafted monolith). This result provided clear evidence that the grafting polymerization of BMA on the surface of the monolith by in-situ ATRP was successful.

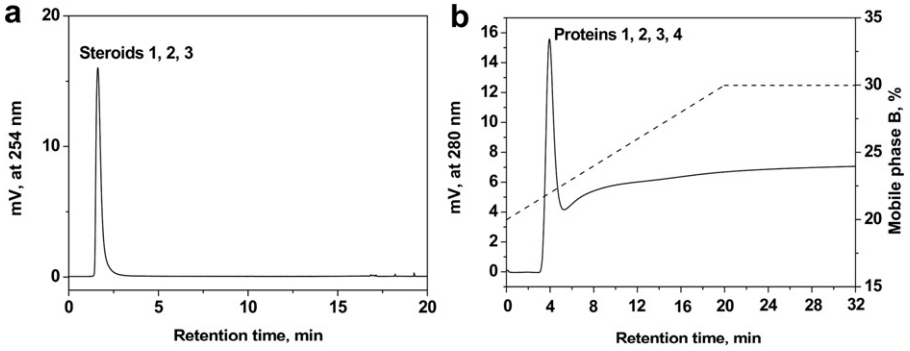

Fig. 8. Chromatograms of separation of three steroids (a) and four proteins (b) using the ungrafted monolith. (The conditions were the same as in Figs. 6 and 7).

3.4. Application of the grafted monolith to HPLC

The PBMA-grafted monolith was then applied to be the stationary phase of chromatographic column for separation of some steroids and standard proteins. The steroids with different hydrophobicities were usually used as a probe in the reversed-phase model. They were defined as the logarithm of its partition coefficients in the *n*-octanol/water system (called as log *P* values), including hydrocortisone (log $P = 1.61$), testosterone (log $P = 3.32$) and progesterone (log $P = 3.87$). In the study, the mixture of the three steroids was separated on the PBMA-grafted monolith, and the order of the retention time of each steroid was consistent with its hydrophobicity, respectively (Fig. 6). The results suggested that the surface of the grafted monolith was hydrophobic. Then, using the same monolith, a four-protein mixture was separated under the reversed-phase model, including ribonuclease, cytochrome *c*, myoglobin and ovalbumin (Fig. 7).

The same mixtures were separated on the ungrafted monolith and the results are shown in Fig. 8. The steroids and proteins could not be separated on the unmodified monolith. Therefore, it could be deduced that the PBMA-grafted monolith was better than unmodified monolith on the separation efficiency.

4. Conclusions

The macroporous monolith with 3D bicontinuous skeleton structure was synthesized by *in-situ* ATRP. The ratio of EDMA to EBP had obvious influence on the structure of the monolith resulted from different branches. It had been found that the mechanism of ATRP played an important role in forming the 3D bicontinuous structure of the monolith. The Br group in the surface of the internal pores in the monolith could further initiate polymerization of vinyl monomer. Furthermore, the PBMA-grafted monolith was used to separate steroids and proteins. This method of preparing 3D bicontinuous monolith has some features, such as the mild reaction, simple operation and a wide range of monomers to be selected compared with other methods. Hence, this method will be expected to be extensively spread in preparation of the monolith with 3D bicontinuous skeleton. Meanwhile, that the volume of the monolith by ATRP could be enlarged to be preparative degree also provided another route to preparing large size monolithic column.

Acknowledgements

We gratefully acknowledge the financial support from Ministry of Science and Technology of China (No. 2007CB714504), NSFC (No. 20875091, No. 20675084 and No. No. 20935005) and Chinese Academy of Sciences.

References

[1] Peters EC, Svec F, Fréchet JMJ. Adv Mater 1999;11:1169–81.
[2] Svec F. J Sep Sci 2009;32:3–9.
[3] Gennes PG, editor. Scaling concept of polymer physics. Cornell University Press; 1979. p. 115.
[4] Horak D, Labsky K, Pilar J, Bleha M, Pelzbauer Z, Svec F. Polymer 1993;34:3481–9.
[5] Svec F. J Sep Sci 2004;27:747–66.
[6] Jiang T, Jiskra J, Claessens HA, Cramers CA. J Chromatogr A 2001;923:215–27.
[7] Tsujioka N, Hira N, Aoki S, Tanaka N, Hosoya K. Macromolecules 2005;38:9901–3.
[8] Hosoya K, Hira N, Yamamoto K, Nishimura M, Tanaka N. Anal Chem 2006;78:5729–35.
[9] Tsujioka N, Ishizuka N, Tanaka N, Kubo T, Hosoya K. J Polym Sci Part A: Polym Chem 2008;46:3272–81.
[10] Kanamori K, Nakanishi K, Hanada T. Adv Mater 2006;18:2407–11.
[11] Aoki H, Tanaka N, Kubo T, Hosoya K. J Polym Sci: Part A: Polym Chem 2008;46:4651–73.
[12] Yao CH, Qi L, Jia HY, Xin PY, Yang GL, Chen Y. J Mater Chem 2009;19:767–72.
[13] Patten ET, Matyjaszewski K. Adv Mater 1998;10:901–15.
[14] Kato M, Kamigaito M, Sawamoto M, Higashimura T. Macromolecules 1995;28:1721–3.
[15] Wang J, Matyjaszewski K. J Am Chem Soc 1995;117:5614–5.
[16] Kamigaito M, Ando T, Sawamoto M. Chem Rev 2001;101:3689–746.
[17] Matyjaszewski K, Xia J. Chem Rev 2001;101:2921–90.
[18] Wang AR, Zhu S. J Polym Sci Part A: Polym Chem 2005;43:5710–4.
[19] Kanamori K, Hasegawa J, Nakanishi K, Hanada T. Macromolecules 2008;41:7186–93.
[20] Min K, Jakubowski W, Matyjaszewski K. Macromol Rapid Commun 2006;27:594–8.
[21] Zhang RY, Yang GL, Xin PY, Qi L, Chen Y. J Chromatogr A 2009;1216:2404–11.
[22] Viklund C, Svec F, Fréchet JMJ, Irgum K. Chem Mater 1996;8:744–50.
[23] Viklund C, Pontén E, Glad B, Irgum K, Hörstedt P, Svec F. Chem Mater 1997;9:463–71.
[24] Mihelic I, Koloini T, Podgornik A. J Appl Polym Sci 2003;87:2326–34.
[25] Svec F, Fréchet JMJ. Macromolecules 1995;28:7580–2.
[26] Gao H, Min K, Matyjaszewski K. Macromolecules 2007;40:7763–70.
[27] Peters EC, Svec F, Fréchet JMJ. Chem Mater 1997;9:1898–902.
[28] Danquah MK, Forde GM. J Chromatogr A 2008;1188:227–33.
[29] Yang Y, Yan X, Cui Y, He Q, Li D, Wang A, et al. J Mater Chem 2008;18:5731–7.
[30] Connal LA, Gurr PA, Qiao GG, Solomon DH. J Mater Chem 2005;15:1286–92.
[31] Kong H, Gao C, Yan D. J Mater Chem 2004;14:1401–5.